Neurochirurgie 65 (2019) 357–364

Disponible en ligne sur ScienceDirect www.sciencedirect.com

Elsevier Masson France EM|consulte www.em-consulte.com

Original article

Diagnostic value of fusion of metabolic and structural images for stereotactic biopsy of brain tumors without enhancement after contrast medium injection☆

J. Todeschi[a,*], C. Bund[b], H. Cebula[a], S. Chibbaro[a], B. Lhermitte[c], Y. Pin[d], F. Lefebvre[e], I.J. Namer[b], F. Proust[a]

[a] Department of neurosurgery, hôpital de Hautepierre, hôpitaux universitaires de Strasbourg, 1, avenue Molière, 67200 Strasbourg, France
[b] Department of nuclear medicine, hôpital de Hautepierre, 67200 Strasbourg, France
[c] Department of pathology, hôpital de Hautepierre, 67200 Strasbourg, France
[d] Department of radiotherapy, Centre Paul Strauss, 67065 Strasbourg, France
[e] Department of public health, hôpitaux universitaires, 67200 Strasbourg, France

ARTICLE INFO

Article history:
Received 16 March 2019
Received in revised form 4 July 2019
Accepted 3 August 2019
Available online 24 September 2019

Keywords:
Biopsy target
^{18}F-FDOPA PET
Glioma target
PET-MRI image registration
Brain tumor

ABSTRACT

Background. – The heterogeneous nature of glioma makes it difficult to select a target for stereotactic biopsy that will be representative of grade severity on non-contrast-enhanced lesion imaging. The objective of this study was to evaluate the benefit of fusion of metabolic images (PET 18F-DOPA) with magnetic resonance imaging (MRI) morphological images for cerebral biopsy under stereotactic conditions of glioma without contrast enhancement.

Patients and methods. – This single-center prospective observational study conducted between January 2016 and April 2018 included 20 consecutive patients (mean age: 45 ± 19.5 years; range, 9–80 years) who underwent cerebral biopsy for a tumor without MRI enhancement but with hypermetabolism on ^{18}F-FDOPA PET (positron emission tomography). Standard ^{18}F-FDOPA uptake value (SUV_{max}) was determined for diagnosis of high-grade glioma, with comparison to histomolecular results.

Results. – Histological diagnosis was made in all patients (100%). Samples from hypermetabolism areas revealed high-grade glial tumor in 16 patients (80%). For a SUV_{max} threshold of 1.75, sensitivity was 81.2%, specificity 50%, PPV 86.7% and VPN 40% for diagnosis of high-grade glioma. No significant association between SUV_{max} and histomolecular mutation was found.

Conclusion. – ^{18}F-FDOPA metabolic imaging is an aid in choosing the target to be biopsied under stereotactic conditions in tumors without MR enhancement. Nevertheless, despite good sensitivity, ^{18}F-FDOPA PET is insufficient for definitive diagnosis of high-grade tumor.

1. Abbreviations

PET	positron emission tomography
MRI	magnetic resonance imaging
^{18} F-FDG	^{18}fluoro-deoxy-glucose
^{18} F–DOPA	[18F] fluoro-L-phenylalanine
AA	amino acids
SUV	standardized uptake values
ROC	receiver operating characteristic
Se	sensitivity
Sp	specificity
PPV	positive predictive value
NPV	negative predictive value
IDH	isocitrate dehydrogenase
ATRX	alpha-thalassemia/mental-retardation syndrome X-linked
MGMT	methylguanine methyltransferase
CBV	cerebral blood volume
BBB	blood-brain barrier
MRS	MR spectroscopy

☆ ^{18}F-FDOPA PET in brain biopsy.

* Corresponding author.
E-mail address: julien.tod@gmail.com (J. Todeschi).

https://doi.org/10.1016/j.neuchi.2019.08.002
0028-3770/

2. Introduction

The reliability of cerebral biopsy for tumor characterization can be impaired by many factors: the heterogeneity of gliomas, but also the limitations of conventional brain MRI (magnetic resonance imaging) for identifying aggressive tumor components [1].

About one-third of high-grade gliomas show no enhancement on MRI, particularly in elderly patients [2]. In these tumors, the choice of biopsy target is therefore sometimes problematic. In addition, T2 hypersignal, most often comprising a heterogeneous mixture of tumor and healthy parenchyma, is relatively uninformative [3]. The absence of clear MRI evidence for tumor aggressiveness may lead to underestimation of malignancy [4]. In order to circumvent this obstacle, association with other imaging techniques is necessary [5,6].

Positron emission tomography (PET) is a credible complement, providing additional information on tumor metabolism and cell renewal [7–9]. In addition, the advent of amino-acid tracers, including 3,4-dihydroxy-6- [18F] fluoro-L-phenylalanine (^{18}F-FDOPA), has improved assessment the extent of tumor infiltration compared with glycolytic metabolism tracers (^{18}F-FDG) [3]. The use of multimodal imaging, combining PET with ^{18}F-FDOPA and structural MRI, is therefore a reliable option to improve the representativeness of tumors in stereotactic brain biopsy.

The objective of this study was to evaluate the benefit of the fusion of metabolic images (PET ^{18}F-FDOPA) with morphological MRI images for brain biopsy under stereotactic glioma conditions without contrast enhancement.

3. Patients and methods

3.1. Study design

This single-center prospective observational study included 20 consecutive patients: mean age: 45 ± 19.5 years (range, 9–80 years); M/F sex ratio, 0.6). Data were collected over a 27-month period at the University Hospital of Strasbourg (France) between January 2016 and April 2018. All patients with glial-like brain tumor, newly diagnosed or with doubt as to malignant transformation, without MRI enhancement after gadolinium injection but with hypermetabolism on 18F-FDOPA PET, were included. Patients in whom first-line surgical resection was feasible were excluded. After multidisciplinary team discussion, biopsy was recommended before surgical resection in patients where there was diagnostic doubt. Informed consent, after oral information, was obtained for each patient before performing the biopsy.

The study objectives were to evaluate the benefit of metabolic imaging in brain biopsy and to determine whether ^{18}F-DOPA PET hypermetabolism in newly diagnosed or recurrent glial tumor without MRI enhancement correlated with high tumor grade.

3.2. Magnetic resonance imaging technique

The MRI investigations (Fig. 1: columns 1 and 2) were performed on an MR 1.5 Tesla unit (Avanto, Siemens Medical Systems) before PET CT. The standard brain tumor diagnostic protocol comprised: turboaxial spin-echo proton-density T1, T2 W, SWI, diffusion-weighted, perfusion-weighted and fluid-attenuated axial recovery (FLAIR) sequences and Multiplanar spin-echo T1 W and 3D magnetization-prepared rapid acquisition gradient-echo (MPRAGE) images obtained after intravenous injection of 0.2 mmol/kg gadolinium contrast agent. MR spectroscopy (MRS) was not performed in the standard protocol. Spatial resolution was 1 × 1 × 1 mm for the 3D MPRAGE sequence and 1 × 1 × 5 mm for all the 2D sequences.

3.3. Positron Emission Tomography with ^{18}F-FDOPA

PET examinations (Fig. 1: column 3) were performed on a Siemens mCT Biograph apparatus. 1.5 MBq/kg (0.04 mCi/kg) of ^{18}F-FDOPA (IASOdopa, IASON, Austria) was injected intravenously. No oral carbidopa premedication was used. 15 min 3-D emission acquisition started 30 min after i.v. injection. PET data were reconstructed with and without CT-based attenuation correction by common iterative algorithm (Ordered Subset Expectation Maximization, 2 iterations, 21 subsets, 128 × 128 matrix). For MRI/PET co-registration and image fusion, raw data were transferred to dedicated workstation (E-soft, Siemens Medical Solutions) in DICOM format. MRI and ^{18}F-FDOPA PET data were then loaded in an application that performs fusion by a fully automated volume-based registration algorithm (3D Fusion, Siemens Medical Solutions).

PET images were interpreted by two-experienced nuclear medicine physicians (I.J.N., C.B.,) informed about patient medical history and lesion location. Final interpretation in case of disagreement was made as a consensus reading.

According to qualitative image interpretation, each focus of ^{18}F-FDOPA uptake (outside the striatal binding) above background level was recorded and interpreted as pathological (hypermetabolism, in red on the various projections). For semi-quantitative analysis of ^{18}F-FDOPA uptake, SUV_{max} per focus was employed, determined as: SUV_{max} = [maximum pixel value in tumor (kBq/mL)]/[injected dose (kBq)/patient weight (g)].

Maximum pixel value in the tumor was obtained for a region of interest (ROI) covering the entire tumor on transaxial slices using superposed T1W-gadolinium-enhanced and FLAIR MRI images as reference. A second ROI of the same size was symmetrically placed on the contralateral hemisphere as normal reference brain region, to obtained SUV_{max} $(T/N)_{30}$ ratio.

3.4. Stereotactic planning

Biopsy targeting and trajectory selection used the robot's planning software (Rosa, Zimmer) the day before surgery, based on MR (T1 gadolinium, T2 and FLAIR) images fused with PET CT ^{18}F-FDOPA images. Surgical planning determined a gyral entry point to avoid a path through a groove. The target point was located in the region of greatest hypermetabolism (in red on the projection) after consultation with the nuclear medicine team (Fig. 1).

3.5. Robotic procedure for stereotactic biopsy

All procedures were performed under general anesthesia. The patient's head was secured using a Mayfield headrest (Integra LifeSciences Corporation), attached to the ROSA® robot by a rigid arm to prevent any mechanical movement. Automatic robotic frameless surface recording was based on non-invasive laser measurement [10]. Registration accuracy was checked by the surgeon on the usual anatomical landmarks (canthus, root of the nose, etc.). A sterile field was implemented, and the robotic arm was automatically positioned along the planned path. A 3.2 mm hole was drilled at the point of entry. A Sedan biopsy needle (10 mm sample window, 2 mm diameter, 200 mm length) was placed along the path to the target area. Rosette biopsies (4–8 samples) were then made by rotating the lateral cut needle according to the standard negative pressure technique in the 4 quadrants. In addition, by raising the needle, staged biopsies were performed. When the tumor was too small for staged biopsy, only "rosette" biopsies were performed. Where possible and not harmful, biopsies were performed on the periphery of hypermetabolic areas. After the biopsies, the needle was removed and the skin was closed with a # 4-0 stitch.

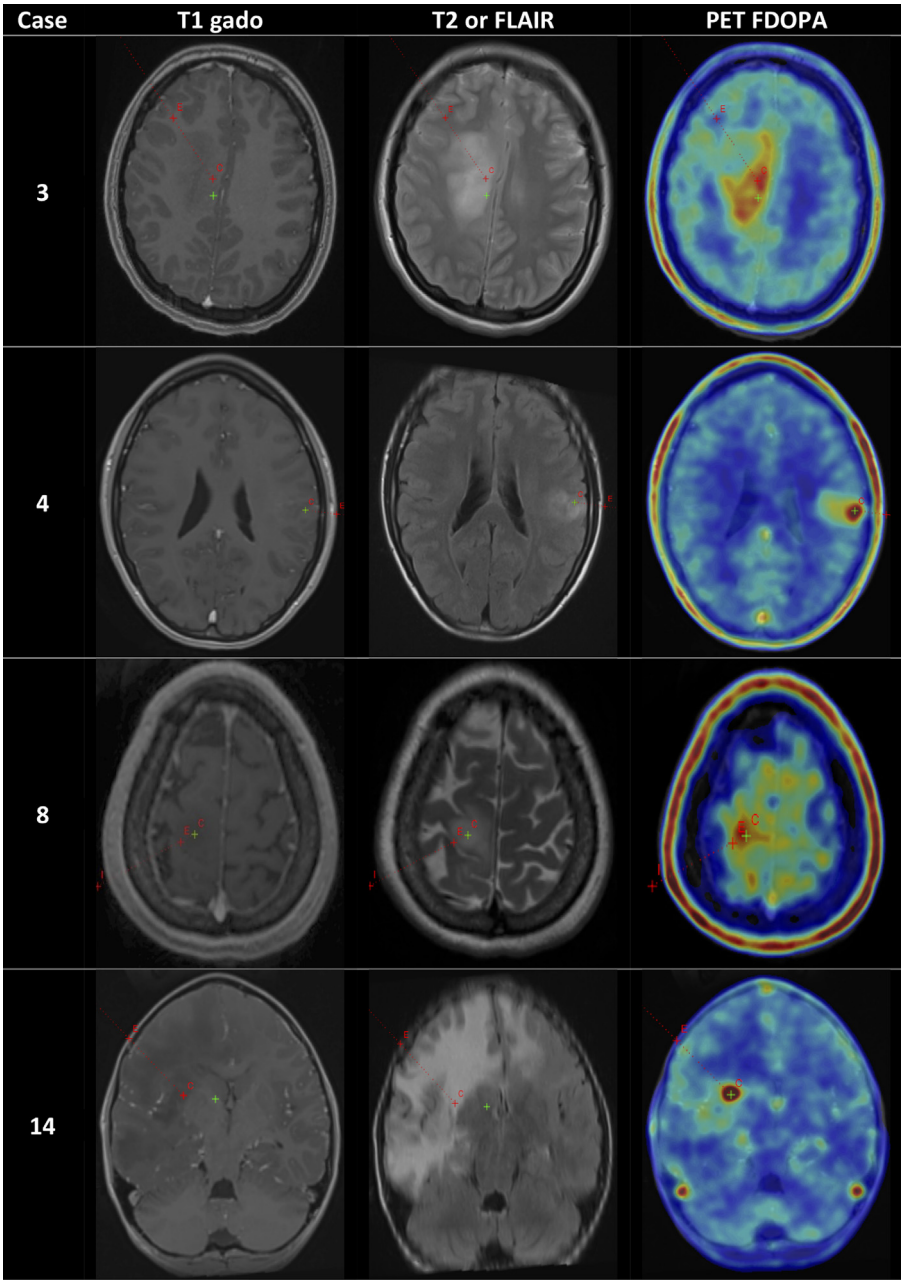

Fig. 1. Examples of ^{18}F-FDOPA PET + brain MRI (T1gadolinium and T2 or FLAIR) fusion using ROSA software (Zimmer) with choice of biopsy target for patients # 3, 4, 5 and 14. Hypermetabolism zones in red on ^{18}F-FDOPA PET images.

3.6. *Postoperative biopsy quality control*

Brain CT was performed in each patient on day 1, with planning analyses to check whether the biopsy site was within the hypermetabolism zone.

Patients were able to return home on D + 1 or 2 postoperatively if clinical status was satisfactory. Pathologic analysis was carried out within 10 days and, after multidisciplinary neuro-oncology team discussion, patients were informed about the proposed treatments.

3.7. *Histopathological and immunohistochemical analysis*

Standard hematoxylin-eosin and Ki67 antibody (MIB-1 clone) staining was performed. IDH1/2 mutation status was analyzed by immunostaining (or direct sequencing) against the R132H common mutation. p53 mutation (by immunostaining), 1p19q codeletion (by gene amplification) and MGMT methylation were screened on a case-by-case basis. Histopathological examination and immunohistochemical data were used for tumor classification according to the WHO 2016 criteria [11]. High-grade glial tumor was diagnosed by combined histological analysis (high cell density, number of mitoses/high fields, endothelial proliferation or presence of necrosis) and immunohistochemical analysis.

3.8. *Diagnostic value of ^{18}F-FDOPA PET*

Histomolecular diagnosis was taken as gold-standard for high-grade glioma. Then a diagnostic threshold SUV_{max} value was determined on ^{18}F-FDOPA PET to optimize sensitivity (Se), specificity (Sp), positive predictive value (PPV) and negative predictive value (NPV). Subsequently, qualitative histological comparison was made between the tumor zone in hypermetabolism and the

peripheral tumor zone outside the hypermetabolism area was performed. Finally, the correlation between SUV_{max} on ^{18}F-FDOPA PET and the histomolecular data (proliferation index KI67, IDH1, 1p19q) was assessed.

3.9. Statistical analysis

Statistical analysis included a descriptive part (quantitative and qualitative variables) and an inferential part (using either χ^2 or Fisher exact test, according to distribution). Quantitative variables were compared between groups either by Student's test (for normal distributions) or else by non-parametric Mann-Whitney-Wilcoxon test. Correlations between quantitative variables were assessed by Pearson correlation coefficient (for normal distributions) or else by Spearman correlation coefficient. A receiver operating characteristic (ROC) curve was drawn with estimates of sensitivity, specificity, and positive and negative predictive values, determining the SUV_{max} threshold for diagnosis of high-grade glioma. The significance threshold was set at 5%; confidence intervals were estimated using the exact method. Analyses used R software, version 3.4.3 (R Foundation for Statistical Computing, Vienna, Austria), and other software packages required for the analyses.

3.10. Ethics

This study was conducted in accordance with the Principles of Ethics for Medical Research Involving Human Subjects set forth in the Declaration of Helsinki and its subsequent amendments. The study was approved by the Strasbourg University Hospitals review board (FC/file 2019-16).

4. Results

4.1. Population characteristics

Twenty patients were included: 8 male, 12 female (sex ratio M/F: 0.6); median age, 45 ± 19.5 years (range, 9–80 years). Sixteen patients had a newly diagnosed tumor; 4 had recurrence of a low-grade glial tumor. Biopsy locations were frontal in 10 patients, parietal in 4, insular in 2, and brain stem (protuberance), hippocampus, temporal lobe and corpus callosum in 1 each. In addition, 5 patients had diffuse brain gliomatosis (Table 1).

Postoperatively, there was no mortality or morbidity (hemorrhagic, infectious or neurologic) related to the stereotactic biopsy procedure. Recalibration between the postoperative brain CT scan and the preoperative planning MRI + PET images systematically confirmed that biopsies were performed in the target hypermetabolism area.

Neuropathology indicated high-grade glioma in 16 patients (80%) (8 anaplastic astrocytomas, 6 glioblastomas, 1 anaplastic ganglioglioma, 1 oligodendroglioma) and low-grade glioma in 4 (20%) (3 grade II oligodendrogliomas, 1 diffuse astrocytoma II). IDH mutation was found in 12 patients: IDH1 in 11 and IDH 2 in 1. Ki67 proliferation index (MIB-1) was < 5% in low-grade tumors and averaged 19.8% (range, 5–40%) in high-grade tumors. p53 mutation was evaluated in only 8 patients, with rates ranging from < 5% to 100%. Other immunohistochemical data were investigated on a case-by-case basis, with discovery of 1p19q codeletion in 4 patients, ATRX loss in 6 and MGMT promoter methylation in 5.

4.2. Histological comparison

In 12 patients, tumor location allowed biopsy of both "hypermetabolic" and "non-hypermetabolic" tumor zones on ^{18}F-FDOPA PET (Fig. 2). Qualitative pathological comparison favored hypermetabolic zones: increase in cell density with aspect of compact tumor and greater vascularization (Fig. 2). Frequently but less systematically (8/12 patients), Ki67 proliferation index and higher mitotic activity were also highlighted. There was, however no significant difference in tumor grade between the 2 zones.

4.3. ^{18}F-FDOPA PET imaging

All patients underwent ^{18}F-FDOPA PET in the 3 weeks prior to brain biopsy. Fusion between MRI and ^{18}F-FDOPA PET images showed that all areas of hypermetabolism were in T2/FLAIR hypersignal regions. Concordance was less clear between hypermetabolic areas and T1 hypointense regions (Figs. 1 and 2). Samples from hypermetabolism zones suggested high-grade glioma in 16 patients (80%). As detailed in Table 1, SUV_{max} averaged 2.18 (range: 1.3–4.1) for high-grade and 2.025 (range: 1.7–2.7) for low-grade tumors, without significant difference ($P = 0.64$; 95%CI [−0.632; 0.9445]). Taking a SUV_{max} threshold at 1.75 (determined on ROC curve), sensitivity was 81.2%, specificity 50%, PPV 86.7% and NPV 40% for diagnosis of high-grade glioma. Area under the curve (AUC) (Fig. 3) was 56.2% (range, 18.1–94.4%); $P = 0.75$. There was no significant association between proliferation index (Ki67) and SUV_{max} ($P = 0.76$) (Fig. 4), or between SUV_{max} and IDH mutation ($P = 0.6$) or 1p19q codeletion ($P = 0.6$). However, patients with ^{18}F-FDOPA PET hypermetabolism without 1p19q codeletion were more likely to have high-grade tumor ($P = 0.013$) (Table 2).

5. Discussion

Samples taken from hypermetabolism zones revealed high-grade glial tumor in 16 patients (80%). Taking a SUV_{max} cut-off value of 1.75 gave Se 81.2%, Sp 50%, PPV 86.7% and NPV 40% for diagnosis of high-grade glioma. There was no significant association between SUV_{max} and histomolecular data.

5.1. Limitations of MRI

Conventional MRI alone has limited sensitivity and specificity to determine glial tumor grade [12]. One of the main reasons is the frequent preservation of the blood-brain barrier [12,13]. Tumor evaluation is based essentially on T2-weighted and FLAIR sequences; however, the latter do not allow reliable discrimination between tumor infiltration, peritumoral vasogenic edema and changes related to treatment potential [14,15]. In addition, very little information can be collected regarding intra-lesional histological heterogeneity, biological activity, or disease aggressiveness. Choice of biopsy target is thus difficult, with results only for the sampled part of the tumor, which can be inaccurate when samples do not concern the most active areas and therefore cannot guide appropriate treatment [16].

5.2. MR spectroscopy (MRS)

MR spectroscopy (MRS) can map metabolite profiles in a defined volume of cerebral parenchyma. Frequently used in first line, it allows differentiation between low- and high-grade tumor by calculating Cho/Cr and Cho/N-acetylaspartate ratios; for example, a tissue regions with elevated Cho is a potential indicator of aggressive tumor [17]. For biopsy, the problem is that spectroscopy generates biochemical maps lacking structural features [1], not allowing MRS to be used for image fusion with structural MRI (rigid body recording methods) in current practice, unlike PET-Scan.

5.3. Interest of PET

In the context of ambiguous MRI findings, molecular imaging may provide additional relevant information on tumor metabolism

Table 1
Demographics and ^{18}F-FDOPA PET results, with calculation of SUV_{max}, in the 20 patients of the cohort.

Nº	Gender/Age	Tumor recurrence	Gliomatosis	Biopsy location	PET F-FDOPA SUV_{MAX}
1	F/27	–	–	Right parietal	2.3
2	F/42	–	Yes	Left frontal	1.9
3	F/17	–	–	Right frontal	1.8
4	F/20	–	–	Left parietal	1.9
5	M/42	–	–	Left parietal	1.8
6	F/58	–	Yes	Corpus callosum	2.5
7	F/80	–	–	Left frontal	2.6
8	M/45	–	–	Right frontal	1.5
9	F/32	Yes	–	Right parietal	2.0
10	F/66	–	–	Right frontal	1.3
11	M/62	–	Yes	Right frontal	2.2
12	M/51	–	–	Protuberance	2.0
13	M/37	–	Yes	Right frontal	1.7
14	M/9	–	Yes	Right frontal	1.6
15	M/69	–	–	Insular	2.2
16	F/50	Yes	–	Left frontal	4.1
17	F/39	Yes	–	Right frontal	2.6
18	F/45	Yes	–	Insular	2.7
19	F/69	–	–	Left hippocampus	1.5
20	M/70	–	–	Left temporal	2.8

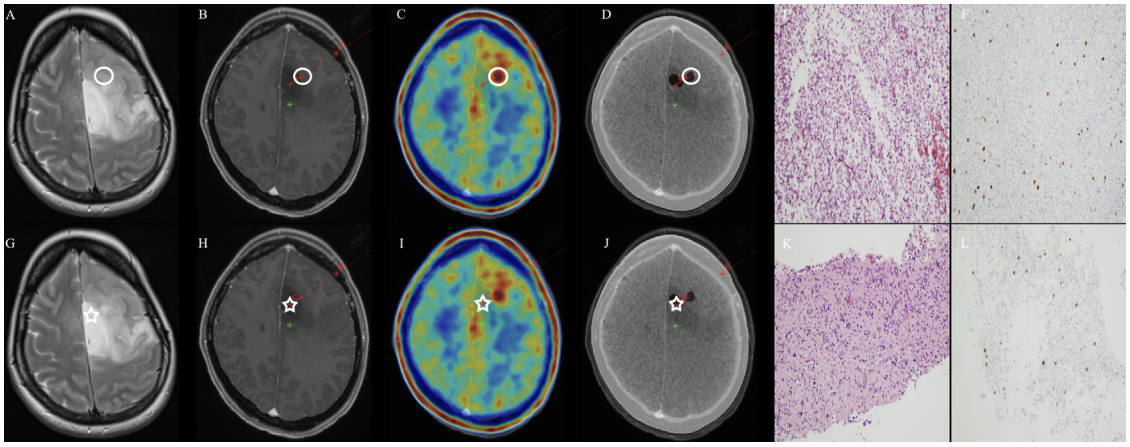

Fig. 2. Example of patient nº 2. White circle: location of biopsies in the hypermetabolic tumor zone (in red on the projection): on MRI (A), FLAIR gadolinium (B), T1 gadolinium (C), ^{18}F-FDOPA PET (D). Postoperative CT with visualization of higher cell density in HE (E), and higher proliferation index (F). White star: location of biopsies in non-hypermetabolic tumor zone: on MRI (G), FLAIR gadolinium (H), T1 gadolinium (I), PET ^{18}F-FDOPA (J). Postoperative CT with visualization of lower cell density in HE (K), and lower proliferation index (L).

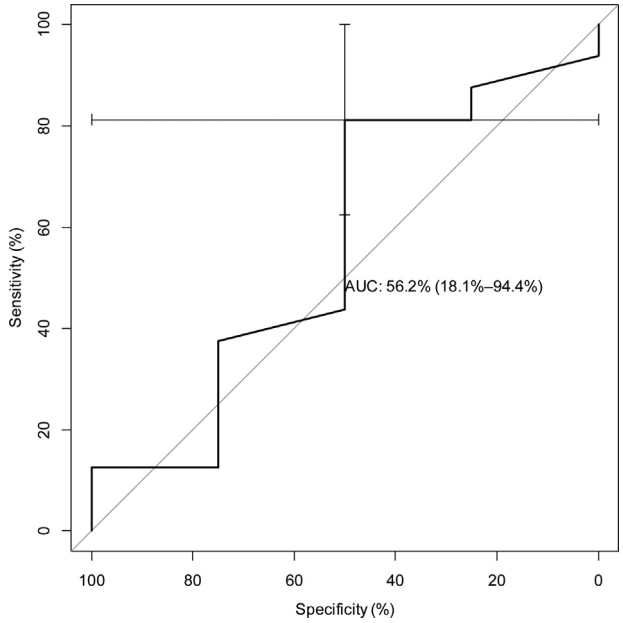

Fig. 3. ROC curve comparing SUV_{max} versus histological lesion grade.

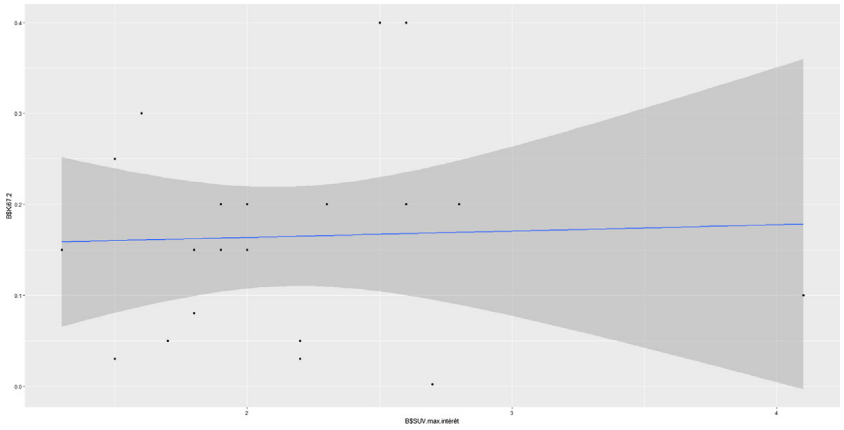

Fig. 4. Proliferation index (Ki67) according to SUV_{max} on ^{18}F-FDOPA PET, showing no significant association.

Table 2
Pathological and immunohistochemical results of the 20 patients of the cohort.

N°	Histology	IDH 1 mutated	1p19qco dElEtion	ATRX loss	MGMT methylation	Ki67%	p53 mutation	Other
1	Anaplastic astrocytoma	Yes	–	Yes	–	20%	10%	
2	Anaplastic astrocytoma	Yes	–	Yes	–	15%	20%	
3	Anaplastic astrocytoma	–	–	Yes	–	15%	30%	
4	Anaplastic ganglioglioma	–	–	–	–	20%	–	BRAF V600E +
5	Anaplastic astrocytoma	Yes	–	Yes	–	8%	–	
6	Glioblastoma	–	–	–	–	40%	–	
7	Glioblastoma	–	–	–	Yes	20%	< 5%	
8	Anaplastic astrocytoma	Yes	–	–	–	25%	100%	
9	Anaplastic astrocytoma	Yes	–	Yes	Yes	15%	60%	
10	Glioblastoma	–	–	–	Yes	15%	–	
11	Anaplastic astrocytoma	–	–	–	–	5%	–	
12	Glioblastoma	–	–	–	–	20%	–	IDH2 +
13	Oligodendroglioma II	Yes	Yes	–	–	5%	–	
14	Anaplastic astrocytoma	Yes	–	–	Yes	30%	–	
15	Oligodendroglioma II	Yes	Yes	–	–	3%	–	
16	Glioblastoma	Yes	–	Yes	–	10%	50%	
17	Anaplastic oligodendroglioma	Yes	Yes	–	–	40%	< 5%	
18	Oligodendroglioma II	Yes	Yes	–	Yes	< 5%	–	
19	Diffuse astrocytoma II	–	–	–	–	3%	–	
20	Glioblastoma	–	–	–	–	20%	–	

and may be useful for clinical decision-making [18]. Moreover, this technique is one of the most promising for the identification and interpretation of tumor expansion, in comparison with rCBV mapping on MRI. [19]. PET imaging uses biologically active tracers labeled with positron-emitting isotopes at micromolar or nanomolar concentrations and relatively short half-lives. Thus, ^{18}F-FDG or a radiolabeled amino acid (AA), which make it possible to identify the tumor regions with increasing proliferation, could be used in association with MRI to identify high-grade tumor components. The three main radiolabeled amino acids used in brain tumor imaging are ^{11}C-methionine (^{11}C-MET), 18F-fluoro-ethyl-L-tyrosine (^{18}F-FET), 3,4-dihydroxy-6- [18F] fluoro-L-phenylalanine (^{18}F-FDOPA) [12,18]. The advantage of these radiolabeled amino acids is that absorption correlates with cell density rather than rupture of the blood-brain barrier (BBB) [13]. Moreover, the various studies of these AAs showed similar results for tumor visualization, extension delineation and metabolically active volume [20–23]. The major disadvantage of ^{11}C-MET is its short half-life (~ 20 min) [20], whereas ^{18}F-FET and ^{18}F-FDOPA have longer half-lives (~ 110 min) and can be used in clinical routine without the need for an on-site cyclotron [18]. The main difference between these 2 tracers is the specific absorption of ^{18}F-FDOPA in the putamen and caudate nucleus, with resulting difficulty in identifying tumors adjacent to the striatum but also the advantage of better stratifying tumor absorption rates compared to background levels in the striatum. In the present study, there were no tumors near the basal ganglia, and this difficulty did not arise.

5.4. Interest of AA tracers in identifying aggressive tumor components

Some studies evaluating ^{18}F-FDOPA indicated that its sensitivity for the detection of low- or high- grade tumors was 96%, versus 61% for ^{18}F-FDG [24,25]. With ^{18}F-FDG, identifying tumors with moderately increased glucose metabolism (low-grade and some high-grade gliomas) may be difficult due to the physiologically high carbohydrate metabolism rate in normal brain tissue [26]. In comparison, AA tracers have better sensitivity, because: 1) they show lower absorption in normal brain tissue than metabolic tracers [24,26,27]; and 2) their transport is generally increased in malignant transformation due to AA flow to tumor tissue, intrinsic AA transporter activity and intracellular AA metabolism rate [28,29]. In addition, uptake may be visualized on PET using AA tracers in tumors not showing enhancement on MRI, because AAs are actively transported across an intact blood-brain barriers, whereas contrast medium can accumulate only when the BBB is ruptured [3].

The absorption density of AA tracers can also be informative on tumor aggressiveness. Morana et al. compared 2 patients with similar histological data and tumor extension but with more severe clinical course and biological tumor behavior in the patient with a

marked increase in AA tracer absorption [12]. This underlines the fact that histology may underestimate the true nature of the tumor if the samples are not taken in the most metabolically active area.

In addition, Pafundi et al. [3], using ^{18}F-FDOPA PET imaging, have defined an optimal SUV_{max} threshold of > 2 to reliably differentiate high-grade astrocytoma zones. In the present series, a > 1.75 SUV_{max} threshold showed better yield for diagnosis of high-grade glial tumor.

5.5. Particularities according to histomolecular type

In the present study, 4 patients with ^{18}F-FDOPA hypermetabolism had an anatomopathological result in favor of grade II glioma, 3 of which were oligodendroglial. These results are in agreement with data from the literature that showed greater absorption of AA tracers (FET [30], MET [31] and ^{18}F-FDOPA [3]) in oligodendrogliomas (1p19q codeletion) despite their better prognosis than astrocytomas of the same grade [30,32]. By extrapolation, Bette et al., concluded that, in low-grade glioma, absence of AA tracer absorption excludes oligodendroglial tumor components while high tracer uptake does not have elevated PPV in favor of oligodendroglial tumor [33]. This is the main reason why AA PET is only 70–80% accurate, according to the literature, in predicting high-grade glioma [34–36]. In addition, ^{18}F-FDOPA PET/MRI fusion was shown to be a reliable imaging biomarker of pediatric infiltrating astrocytoma, with a relevant diagnostic contribution of 69% [12]. The present study is consistent with these findings, predicting 80% of high-grade gliomas. However, even with a SUV_{max} threshold of 1.75, specificity and NPV remain low, mainly because of the small sample size (20 patients) but also due to 3 low-grade oligodendroglial tumors in the series. Also, it seems that ^{18}F-FDOPA PET cannot by itself predict the histomolecular status of a patient. Bette et al. found no association between static ^{18}F-FET PET and other histopathological markers such as IDH1 or 2 mutation, proliferation index or p53 mutation [33]. Our results with ^{18}F-FDOPA PET are in line with those reported in the literature, with no significant association between SUV_{max} and Ki67 or IDH mutation.

AA PET therefore does not allow completely reliable glioma grade prediction, due to very variable absorption according to WHO histological type [37].

5.6. Study limitations

The absence of tumor grade difference between biopsies in zones of hypermetabolism and non-hypermetabolism can be explained by the proximity of the two sampling zones and by the choice of a single biopsy trajectory. This could skew the classification and lead to significant interpretation bias.

The relative unavailability of ^{18}F-FDOPA PET and its high implementation cost are the most important limitations for these biopsies. Moreover, it is a radioactive substance, the use of which is controlled. As previously discussed, using an ^{18}F-FDOPA AA tracer can complicate the evaluation of tumors located near the basal ganglia, due to physiological absorption into the striata [18]. For biopsy, image fusion with 3D MRI sequences is essential, particularly because of the lower spatial resolution of PET, around 4 mm compared to 1–2 mm for MRI.

6. Conclusion

Despite limited accessibility, ^{18}F-FDOPA PET in tumors without MRI enhancement optimizes the choice of brain biopsy targets under stereotactic conditions of structurally heterogeneous tumors. Fusion with MRI can significantly improve the diagnostic yield and the representativeness of these tumors, better guiding therapeutic strategy. Despite good sensitivity, ^{18}F-FDOPA PET is currently unable to establish a reliable tumor grade.

Ethical statement

All procedures performed in studies involving human participants were in accordance with the ethical standards of the institutional and/or national research committee and with the 1964 Helsinki Declaration and its later amendments or comparable ethical standards.

Informed consent

Informed consent was obtained from all individual participants included in the study.

Funding

No funding was received for this research.

Disclosure of interest

The authors declare that they have no competing interest.

References

[1] Grech-Sollars M, Vaqas B, Thompson G, Barwick T, Honeyfield L, O'Neill K, et al. An MRS- and PET-guided biopsy tool for intraoperative neuronavigational systems. J Neurosurg 2017;127:709–964.
[2] Scott JN, Brasher PM, Sevick RJ, Rewcastle NB, Forsyth PA. How often are nonenhancing supratentorial gliomas malignant? A population study. Neurology 2002;59:947–9.
[3] Pafundi DH, Laack NN, Youland RS, Parney IF, Lowe VJ, Giannini C, et al. Biopsy validation of 18F-DOPA PET and biodistribution in gliomas for neurosurgical planning and radiotherapy target delineation: results of a prospective pilot study. Neuro Oncol 2013;15:1058–67.
[4] Jackson RJ, Fuller GN, Abi-Said D, Lang FF, Gokaslan ZL, Shi WM, et al. Limitations of stereotactic biopsy in the initial management of gliomas. Neuro Oncol 2001;3:193–200.
[5] Tanaka Y, Nariai T, Momose T, Aoyagi M, Maehara T, Tomori T, et al. Glioma surgery using a multimodal navigation system with integrated metabolic images. J Neurosurg 2009;110:163–72.
[6] Mert A, Kiesel B, Wohrer A, Martinez-Moreno M, Minchev G, Furtner J, et al. Introduction of a standardized multimodality image protocol for navigation-guided surgery of suspected low-grade gliomas. Neurosurg Focus 2015;38:E4.
[7] Levivier M, Goldman S, Pirotte B, Brucher JM, Baleriaux D, Luxen A, et al. Diagnostic yield of stereotactic brain biopsy guided by positron emission tomography with [18F]fluorodeoxyglucose. J Neurosurg 1995;82:445–52.
[8] Misch M, Guggemos A, Driever PH, Koch A, Grosse F, Steffen IG, et al. (18)F-FET-PET guided surgical biopsy and resection in children and adolescence with brain tumors. Childs Nerv Syst 2015;31:261–7.
[9] Pirotte B, Goldman S, Dewitte O, Massager N, Wikler D, Lefranc F, et al. Integrated positron emission tomography and magnetic resonance imaging-guided resection of brain tumors: a report of 103 consecutive procedures. J Neurosurg 2006;104:238–53.
[10] Coca HA, Cebula H, Benmekhbi M, Chenard MP, Entz-Werle N, Proust F. Diffuse intrinsic pontine gliomas in children: Interest of robotic frameless assisted biopsy. A technical note. Neurochirurgie 2016;62:327–31.
[11] Louis DN, Perry A, Reifenberger G, von Deimling A, Figarella-Branger D, Cavenee WK, et al. The 2016 World Health Organization Classification of Tumors of the Central Nervous System: a summary. Acta Neuropathol 2016;131:803–20.
[12] Morana G, Piccardo A, Milanaccio C, Puntoni M, Nozza P, Cama A, et al. Value of 18F-3,4-dihydroxyphenylalanine PET/MR image fusion in pediatric supratentorial infiltrative astrocytomas: a prospective pilot study. J Nucl Med 2014;55:718–23.
[13] Bund C, Heimburger C, Imperiale A, Lhermitte B, Chenard MP, Lefebvre F, et al. FDOPA PET-CT of nonenhancing brain tumors. Clin Nucl Med 2017;42:250–7.
[14] Schomas DA, Laack NN, Rao RD, Meyer FB, Shaw EG, O'Neill BP, et al. Intracranial low-grade gliomas in adults: 30-year experience with long-term follow-up at Mayo Clinic. Neuro Oncol 2009;11:437–45.
[15] Grosu AL, Feldmann H, Dick S, Dzewas B, Nieder C, Gumprecht H, et al. Implications of IMT-SPECT for postoperative radiotherapy planning in patients with gliomas. Int J Radiat Oncol Biol Phys 2002;54:842–54.
[16] Kleihues P, Cavenee WK. Pathology and Genetics of Tumors of the Nervous System. Lyon, France: IARC Press; 2000.
[17] Tong T, Yang Z, Chen JW, Zhu J, Yao Z. Dynamic 1H-MRS assessment of brain tumors: a novel approach for differential diagnosis of glioma. Oncotarget 2015;6:32257–65.

[18] Galldiks N, Langen KJ, Pope WB. From the clinician's point of view - What is the status quo of positron emission tomography in patients with brain tumors? Neuro Oncol 2015;17:1434–44.
[19] Filss CP, Cicone F, Shah NJ, Galldiks N, Langen KJ. Amino acid PET and MR perfusion imaging in brain tumours. Clin Transl Imaging 2017;5:209–23.
[20] Becherer A, Karanikas G, Szabo M, Zettinig G, Asenbaum S, Marosi C, et al. Brain tumour imaging with PET: a comparison between [18F]fluorodopa and [11C]methionine. Eur J Nucl Med Mol Imaging 2003;30:1561–7.
[21] Grosu AL, Astner ST, Riedel E, Nieder C, Wiedenmann N, Heinemann F, et al. An interindividual comparison of O-(2-[18F]fluoroethyl)-L-tyrosine (FET)- and L-[methyl-11C]methionine (MET)-PET in patients with brain gliomas and metastases. Int J Radiat Oncol Biol Phys 2011;81:1049–58.
[22] Kratochwil C, Combs SE, Leotta K, Afshar-Oromieh A, Rieken S, Debus J, et al. Intra-individual comparison of (1)(8)F-FET and (1)(8)F-DOPA in PET imaging of recurrent brain tumors. Neuro Oncol 2014;16:434–40.
[23] Lapa C, Linsenmann T, Monoranu CM, Samnick S, Buck AK, Bluemel C, et al. Comparison of the amino acid tracers 18F-FET and 18F-DOPA in high-grade glioma patients. J Nucl Med 2014;55:1611–6.
[24] Chen W, Silverman DH, Delaloye S, Czernin J, Kamdar N, Pope W, et al. 18F-FDOPA PET imaging of brain tumors: comparison study with 18F-FDG PET and evaluation of diagnostic accuracy. J Nucl Med 2006;47:904–11.
[25] Hustinx R, Smith RJ, Benard F, Bhatnagar A, Alavi A. Can the standardized uptake value characterize primary brain tumors on FDG-PET? Eur J Nucl Med 1999;26:1501–9.
[26] Wong TZ, van der Westhuizen GJ, Coleman RE. Positron emission tomography imaging of brain tumors. Neuroimaging Clin N Am 2002;12:615–26.
[27] Ledezma CJ, Chen W, Sai V, Freitas B, Cloughesy T, Czernin J, et al. 18F-FDOPA PET/MRI fusion in patients with primary/recurrent gliomas: initial experience. Eur J Radiol 2009;71:242–8.
[28] Isselbacher KJ. Sugar and amino acid transport by cells in culture–differences between normal and malignant cells. N Engl J Med 1972;286:929–33.
[29] Busch H, Davis JR, Honig GR, Anderson DC, Nair PV, Nyhan WL. The uptake of a variety of amino acids into nuclear proteins of tumors and other tissues. Cancer Res 1959;19:1030–9.
[30] Jansen NL, Schwartz C, Graute V, Eigenbrod S, Lutz J, Egensperger R, et al. Prediction of oligodendroglial histology and LOH 1p/19q using dynamic [(18)F]FET-PET imaging in intracranial WHO grade II and III gliomas. Neuro Oncol 2012;14:1473–80.
[31] Shinozaki N, Uchino Y, Yoshikawa K, Matsutani T, Hasegawa A, Saeki N, et al. Discrimination between low-grade oligodendrogliomas and diffuse astrocytoma with the aid of 11C-methionine positron emission tomography. J Neurosurg 2011;114:1640–7.
[32] Manabe O, Hattori N, Yamaguchi S, Hirata K, Kobayashi K, Terasaka S, et al. Oligodendroglial component complicates the prediction of tumour grading with metabolic imaging. Eur J Nucl Med Mol Imaging 2015;42:896–904.
[33] Bette S, Gempt J, Delbridge C, Kirschke JS, Schlegel J, Foerster S, et al. Prognostic Value of O-(2-[18F]-Fluoroethyl)-L-Tyrosine-Positron Emission Tomography Imaging for Histopathologic Characteristics and Progression-Free Survival in Patients with Low-Grade Glioma. World Neurosurg 2016;89:230–9.
[34] Dunet V, Pomoni A, Hottinger A, Nicod-Lalonde M, Prior JO. Performance of 18F-FET versus 18F-FDG-PET for the diagnosis and grading of brain tumors: systematic review and meta-analysis. Neuro Oncol 2016;18:426–34.
[35] Rapp M, Heinzel A, Galldiks N, Stoffels G, Felsberg J, Ewelt C, et al. Diagnostic performance of 18F-FET PET in newly diagnosed cerebral lesions suggestive of glioma. J Nucl Med 2013;54:229–35.
[36] Popperl G, Kreth FW, Mehrkens JH, Herms J, Seelos K, Koch W, et al. FET PET for the evaluation of untreated gliomas: correlation of FET uptake and uptake kinetics with tumour grading. Eur J Nucl Med Mol Imaging 2007;34:1933–42.
[37] Dunet V, Prior JO. Response to: performance of 18F-FET-PET versus 18F-FDG-PET for the diagnosis and grading of brain tumors: inherent bias in meta-analysis not revealed by quality metrics. Neuro Oncol 2016;18:1029–30.